Acta Crystallographica Section D
**Biological Crystallography**
ISSN 0907-4449

# Contamination from an affinity column: an encounter with a new villain in the world of membrane-protein crystallization

**Pankaj Panwar,[a,b,c]‡§ Aurélien Deniaud[a,b,c]‡¶ and Eva Pebay-Peyroula[a,b,c]***

[a]CEA, Institut de Biologie Structurale Jean-Pierre Ebel, 41 Rue Jules Horowitz, 38027 Grenoble, France, [b]CNRS, Institut de Biologie Structurale Jean-Pierre Ebel, 41 Rue Jules Horowitz, 38027 Grenoble, France, and [c]Université Joseph Fourier, Institut de Biologie Structurale Jean-Pierre Ebel, 41 Rue Jules Horowitz, 38027 Grenoble, France

‡ These authors contributed equally to this work.
§ Current affiliation: Department of Biochemistry, University of Alberta, 451 Medical Sciences Building, Edmonton, Alberta, Canada T6G 2H7.
¶ Current affiliation: European Molecular Biology Laboratory, Grenoble Outstation, 38000 Grenoble, France.

Correspondence e-mail: eva.pebay-peyroula@ibs.fr

Received 22 February 2012
Accepted 11 June 2012

**PDB Reference:** streptavidin triple mutant, complex with desthiobiotin, 4dne.

Attempts to crystallize *At*NTT1, a chloroplast ATP/ADP transporter from *Arabidopsis thaliana*, revealed an unexpected contaminant, *Strep*-Tactin, a variant of streptavidin that was used during purification of the protein. Although it was present in very small amounts, crystals of *Strep*-Tactin were reproducibly grown from the *At*NTT1 solution. *At*NTT1 was overexpressed in *Escherichia coli* and purified from detergent-solubilized membrane fractions using *Strep*-Tactin affinity chromatography based on an engineered streptavidin. The contamination of protein solutions purified on *Strep*-Tactin columns has never been described previously and seems to be specific to membrane proteins solubilized in detergents. Trace amounts of *Strep*-Tactin were observed to be eluted from a *Strep*-Tactin column using several routinely used detergents, illustrating their possible role in the contamination. This finding raises an alarm and suggests caution in membrane-protein purification using *Strep*-Tactin affinity columns, where detergents are essential components. The small crystals of contaminant protein led to the structure at 1.9 Å resolution of *Strep*-Tactin in complex with desthiobiotin.

## 1. Introduction

Crystallization is a multifactor-dependent process, although protein purity and structural homogeneity are considered to be the most critical factors. Even a trace amount of impurity can interfere with crystallization or can lead to crystals of poor diffraction quality (Caylor *et al.*, 1999). Many of the proteins prepared for structural studies are now overexpressed with tags and their purification is greatly improved with the aid of affinity columns. However, even in the last decades of protein crystallography, the crystallization of target proteins in the presence of contaminants as well as the crystallization of trace amounts of contaminants has been reported several times (Cámara-Artigas *et al.*, 2006; Lohkamp & Dobritzsch, 2008; Contreras-Martel *et al.*, 2006). Among all proteins, membrane proteins remain particularly difficult to produce and crystallize. The presence of contaminants that crystallize easily is a major obstacle when screening the crystallization conditions. As an example, AcrB, a multidrug-efflux pump that is located in the plasmic membrane of *Escherichia coli*, is easily co-purified with His-tagged overexpressed membrane proteins purified by metal-affinity chromotagraphy and crystallizes even when present in trace quantities (Veesler *et al.*, 2008). *Strep*-tagged membrane proteins exhibit a higher specificity

for engineered streptavidin matrices (Schmidt & Skerra, 1994; Voss & Skerra, 1997) and can thus be better purified, as shown previously by our group and others (Deniaud *et al.*, 2009). In order to crystallize *At*NTT1 for structural studies, the protein was purified by two-step affinity chromatography including a *Strep*-Tactin matrix. *Strep*-Tactin is a genetically engineered variant of streptavidin with improved peptide-binding capacity (Voss & Skerra, 1997; Schmidt & Skerra, 2007). Unexpectedly, *Strep*-Tactin crystals were obtained. To the best of our knowledge, this is the first report describing the crystallization of a contaminant derived from an affinity column. These crystals led to the first structure of the complex between the engineered streptavidin and the biotin analogue desthiobiotin.

## 2. Methods

### 2.1. Expression and purification of *At*NTT1

*At*NTT1 (UniProt sequence No. Q39002) lacking the first 79 residues corresponding to the N-terminal transit peptide, but containing an N-terminal His tag and a C-terminal *Strep*-tag II, was expressed and purified as described previously (Deniaud *et al.*, 2011, 2012). Briefly, the protein was overexpressed in *E. coli* C43 cells. For purification of *At*NTT1, membranes were prepared by ultracentrifugation and solubilized in 50 m*M* Tris pH 8, 100 m*M* NaCl, 1%(*w*/*v*) lauryl-amidodimethylpropylaminoxide (LAPAO), 10 m*M* imidazole and one tablet of EDTA-free Complete protease inhibitor (Roche) per 50 ml. Extracted proteins were applied in batches onto Ni–NTA beads (Qiagen) for 2 h. The resin was washed before elution with 200 m*M* imidazole. After desalting, Ni-purified proteins were incubated overnight with *Strep*-Tactin beads (IBA). After washing, proteins were eluted in 20 m*M* Tris pH 8, 100 m*M* NaCl, 0.1%(*w*/*v*) LAPAO, 3 m*M* desthiobiotin. The buffer was exchanged to 20 m*M* Tris pH 8, 10 m*M* NaCl, 0.1%(*w*/*v*) LAPAO using a PD10 desalting column (GE Healthcare). Finally, pure proteins were concentrated on an Amicon concentrator with a 50 kDa cutoff before crystallization.

### 2.2. Crystallization, data collection and structure determination

*At*NTT1 concentrations ranged from 5 to 10 mg ml$^{-1}$. As it is a contaminant, the concentration of *Strep*-Tactin in the crystallizations setups is difficult to estimate. However, *Strep*-Tactin crystals appeared in one of the two phases during, or close to, a phase separation, meaning that the initially very low concentration of *Strep*-Tactin is most probably increased in this step. Crystallization screening was performed using a vapour-diffusion setup in 96-well plates by mixing 100 nl protein solution with an equal amount of reservoir solution (100 µl of a commercial screening condition; Qiagen) at 293 K (HTX platform, EMBL Grenoble/PSB). Crystals obtained in 0.01 *M* magnesium sulfate, 50 m*M* sodium cacodylate pH 6.5, 2 *M* ammonium sulfate were flash-cooled in liquid nitrogen in the presence of 30%(*v*/*v*) glycerol as a cryoprotectant. When crystallization was repeated manually, 1 µl drops were equilibrated over 500 µl reservoirs. Diffraction data were collected at 100 K on beamline ID14eh1 at the ESRF, Grenoble and

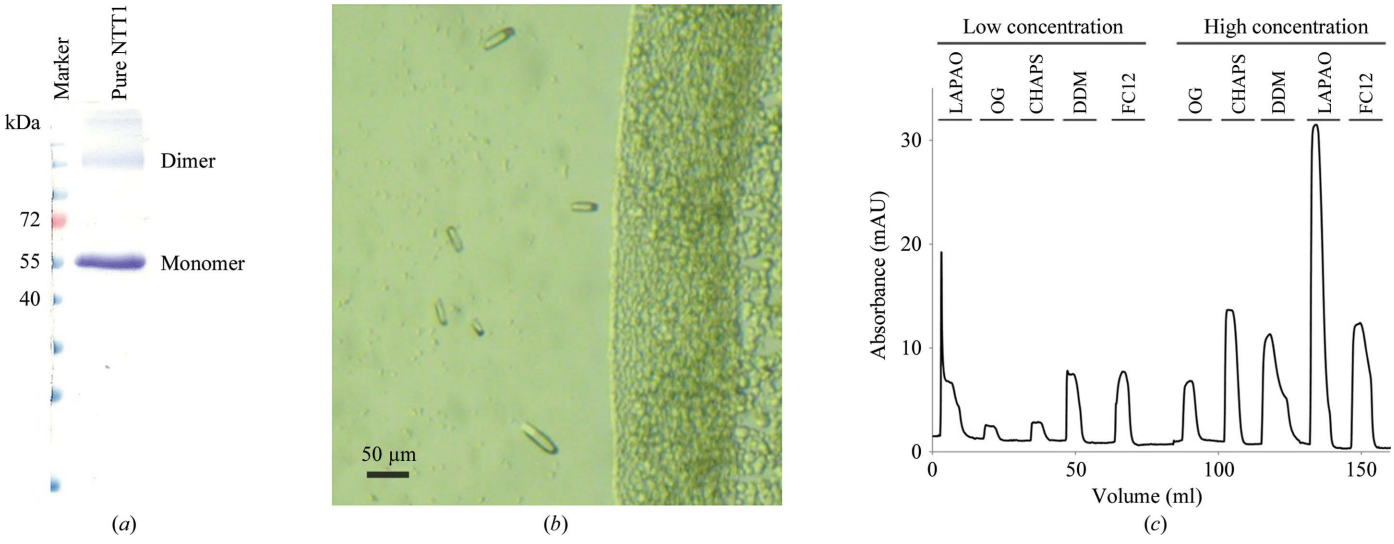


(*a*) (*b*) (*c*)

**Figure 1**
(*a*) SDS–PAGE of *At*NTT1 solution after two-step purification. The main band corresponds to the expected molecular weight of *At*NTT1 and a second faint band corresponds to an *At*NTT1 dimer. No bands at molecular weights of 19, 38 or 76 kDa corresponding to *Strep*-Tactin monomers, dimers or tetramers, respectively, are visible. (*b*) *Strep*-Tactin crystals. The figure represents a portion of the crystallization drop and highlights the phase separation occurring in the drop. The right part (central part of the drop) contains a strong precipitate, while *Strep*-Tactin crystals (seen on the left) grow within the outer shell of the drop. The typical length of the crystals shown in the picture is 50 µm. (*c*) Release of *Strep*-Tactin from *Strep*-Tactin beads in the presence of detergents. UV chromatogram revealing the presence of *Strep*-Tactin released from the beads in the presence of the following detergents: 0.1%(*w*/*v*) LAPAO, 0.2%(*w*/*v*) octylglucoside (OG), 0.1%(*w*/*v*) CHAPS, 0.05%(*w*/*v*) dodecylmaltoside (DDM), 0.1%(*w*/*v*) Fos-Choline 12 (FC12), 1%(*w*/*v*) OG, 1%(*w*/*v*) CHAPS, 1%(*w*/*v*) DDM, 1%(*w*/*v*) LAPAO and 1%(*w*/*v*) FC12.

**Table 1**
Statistics of data collection, processing and structure refinement.

Values in parentheses are for the highest resolution shell.

| | |
|---|---|
| Data collection and processing | |
| Diffraction source | Beamline ID14eh1, ESRF Grenoble |
| Wavelength (Å) | 0.9334 |
| Temperature (K) | 100 |
| Detector | ADSC Quantum 210 |
| Rotation range per image (°) | 1 |
| Total rotation range (°) | 251 |
| Space group | *I*222 |
| Unit-cell parameters (Å, °) | $a$ = 46.72, $b$ = 93.78, $c$ = 104.41, $\alpha = \beta = \gamma$ = 90 |
| Resolution range (Å) | 46.86–1.88 (1.98–1.88) |
| No. of unique reflections | 19097 |
| Completeness (%) | 99.5 (96.7) |
| Mean $I/\sigma(I)$ | 5.8 (1.8) |
| Multiplicity | 6.1 (4.3) |
| $R_{\rm merge}$ | 0.12 (0.41) |
| Overall $B$ factor from Wilson plot (Å$^2$) | 12.5 |
| Structure refinement | |
| Resolution range (Å) | 46.86–1.88 (1.93–1.88) |
| Completeness (%) | 99.4 (93.6) |
| No. of reflections (working set) | 17153 (1210) |
| No. of reflections (test set) | 966 (70) |
| $R$ factor/$R_{\rm free}$ (%) | 18.14 (23.50)/21.90 (29.60) |
| R.m.s.d. bond lengths (Å) | 0.0118 |
| R.m.s.d. bond angles (°) | 1.3821 |
| Average $B$ values (Å$^2$) | 15.2 |
| No. of non-H atoms (protein) | 1809 |
| No. of non-H atoms (ligand) | 30 |
| No. of water molecules | 91 |
| No. of atoms (sulfate ions) | 30 |
| Total No. of non-H atoms | 1960 |
| Ramachandran plot (%) | |
| Favoured regions | 90.2 |
| Additionally allowed | 9.8 |
| Outliers | 0 |

were processed with *XDS* (Kabsch, 2010) and programs from the *CCP*4 suite (Winn *et al.*, 2011). The structure was solved by molecular replacement with the program *Phaser* (McCoy *et al.*, 2007) using the polyalanine chain of PDB entry 1mk5 (Hyre *et al.*, 2006) as a starting model. The model was further built and refined with *Coot* (Emsley & Cowtan, 2004) and *REFMAC* (Murshudov *et al.*, 2011), respectively. Data-collection and processing statistics are summarized in Table 1.

### 2.3. Detergent elution of engineered streptavidin from *Strep*-Tactin

A 1 ml *Strep*-Tactin Sepharose High Performance (Strep-Trap) column (GE Healthcare) was used at a flow rate of 1 ml min$^{-1}$. The column was washed sequentially with 10 ml 20 m*M* Tris pH 8, 0.1 *M* NaCl containing different detergents at two different concentrations.

## 3. Results and discussion

### 3.1. Purification and crystallization

The final purity of *At*NTT1 is shown in Fig. 1(*a*). Small crystals appeared from the initial crystallization assays after 2–3 d. The crystals were obtained from different protein batches purified with beads that were used in a few purifications or with freshly prepared beads. When reproduced in larger drops, they clearly appeared at the peripheral region of the drops (Fig. 1*b*) near the consolution boundary that delineates the two immiscible phases obtained when using detergents (Reiss-Husson & Picot, 1999). It is highly probable that phase separation may have assisted in concentrating *Strep*-Tactin into the phase which is poor in detergent, whereas

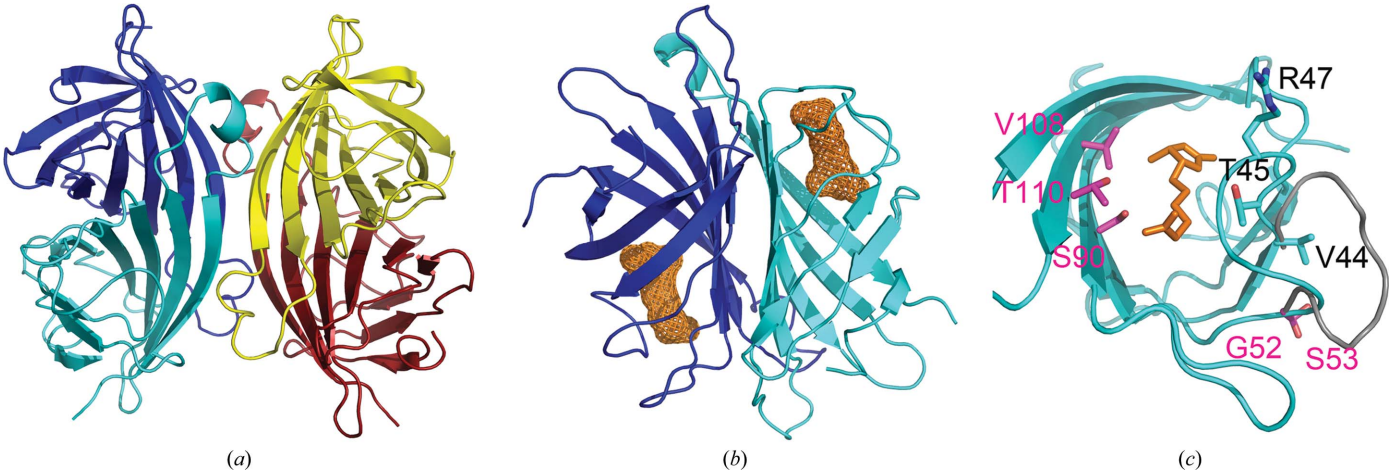


**Figure 2**
The structure of the triple mutant of streptavidin in the presence of desthiobiotin. (*a*) Overall picture showing the tetramer. Monomers in cyan and blue form the dimer that is present in the asymmetric unit; monomers in yellow and red are generated by crystallographic symmetry and constitute the second dimer forming the tetramer. (*b*) Binding sites of desthiobiotin (orange) within the dimer. The colour code for the monomers is the same as in (*a*). (*c*) Binding pocket with three mutations: Glu44Val, Ser45Thr and Val47Arg. The monomer in cyan forms the binding pocket for desthiobiotin. The same protein with the three mutations but in the apo form (shown in grey) adopts an open conformation of the binding site (PDB entry 1kff; Korndörfer & Skerra, 2002). In the presence of *Strep*-tag II (PDB entry 1kl3; Korndörfer & Skerra, 2002) the loop is also open (data not shown). Mutations in streptavidin R7-2 are shown in magenta (PDB entry 3rdq; Magalhães *et al.*, 2011). Desthiobiotin complexed to R7-2 streptavidin superimposes with the ligand in the structure presented here (not shown).

*At*NTT1 amassed in the detergent-rich phase as a precipitate. However, *Strep*-Tactin was not detected in SDS–PAGE analysis (Fig. 1*a*); only N-terminal sequencing of the purified solution revealed low amounts of *Strep*-Tactin in addition to *At*NTT1, the major protein in the solution. In contrast, N-terminal sequencing of dissolved crystals clearly revealed the presence of only engineered streptavidin from *Streptomyces avidinii*.

### 3.2. Structure of the engineered streptavidin bound to desthiobiotin

The best crystals diffracted X-rays isotropically to 1.8 Å resolution. The space group (*I*222) and unit-cell parameters ($a$ = 46.87, $b$ = 94.03, $c$ = 104.60 Å) have been reported previously for several streptavidin structures. The crystals are isomorphous to those used to obtain the structures with PBD codes 1mk5 (Hyre *et al.*, 2006), 1df8 (Hyre *et al.*, 2000) and 2izl (Katz, 1997). The structure was refined at 1.9 Å resolution with an $R$ factor of 18.1% and an $R_{\rm free}$ of 21.9% (Table 1). *Strep*-Tactin forms a tetramer (Fig. 2*a*) generated by crystallographic symmetry from one dimer contained in the asymmetric unit (Fig. 2*b*). Monomers *A* and *B* of the asymmetric unit consist of residues 15–134 and 16–135, respectively, as well as one desthiobiotin molecule per monomer. The structure highlights the three mutations E44V, S45T and V47R localized in the biotin-binding site that were engineered to improve the *Strep*-Tag II binding (Fig. 2*c*). The side chains of these mutated residues were easily identified in the experimental electron-density map.

A large number of streptavidin structures have been deposited in the PDB, either of native streptavidin in the apo form or complexed with biotin or *Strep*-tag II peptides or of streptavidin mutants (see Table 4 in Korndörfer & Skerra, 2002 and, more recently, Chivers *et al.*, 2011). The structure presented here is the only structure of the triple mutant in the presence of desthiobiotin. In general, in the presence of biotin or biotin analogues the binding site of native streptavidin is tightly closed by a loop consisting of residues 45–52, whereas in the apo form or in the presence of *Strep*-Tag II peptide this loop is open and even partially disordered. However, the lid-like loop in known structures of the triple mutant is always in an open conformation (Korndörfer & Skerra, 2002). In contrast, in the presence of desthiobiotin, a biotin analogue, the loop of the triple mutant is in a closed conformation and folds back on the ligand (Fig. 2*c*). The overall structure of the tetramer and the precise details of the binding pocket are very similar to most streptavidin structures that were crystallized in the presence of biotin analogues, with typical r.m.s.d.s on $C^{\alpha}$ atoms in the region of 0.4 Å. The three *Strep*-Tactin mutations do not modify the immediate ligand environment in the binding pocket, as seen in Fig. 3(*a*). Indeed, Thr45 interacts with desthiobiotin in a similar way as Ser45 does with biotin. The role of this mutation cannot be easily understood from the structure. However, a large modification of the cavity results from the Val47Arg mutation. Indeed, the bulky arginine residue prolongs the ridge of the cavity towards the adjacent dimer, as seen in Figs. 3(*b*) and 3(*c*), which compare the cavity of wild-type streptavidin with that of *Strep*-Tactin. In addition, Arg47 forms hydrogen bonds to Trp120 and Asn118, both from the adjacent dimer. Trp120 has been shown to participate in the high binding affinity of biotin by capping the ligand (Chilkoti *et al.*, 1995). Therefore, enhancing the interaction between the two adjacent dimers *via* the interaction of Trp120 and Arg47 might enhance both the ligand binding and the stability of the tetramer. Although residue 44 does not directly interact with the ligand, it can be noticed from the streptavidin–biotin complex that Glu44 is almost within hydrogen-bonding distance of Arg53 (4.2 Å between Glu44 $O^{\varepsilon 2}$ and

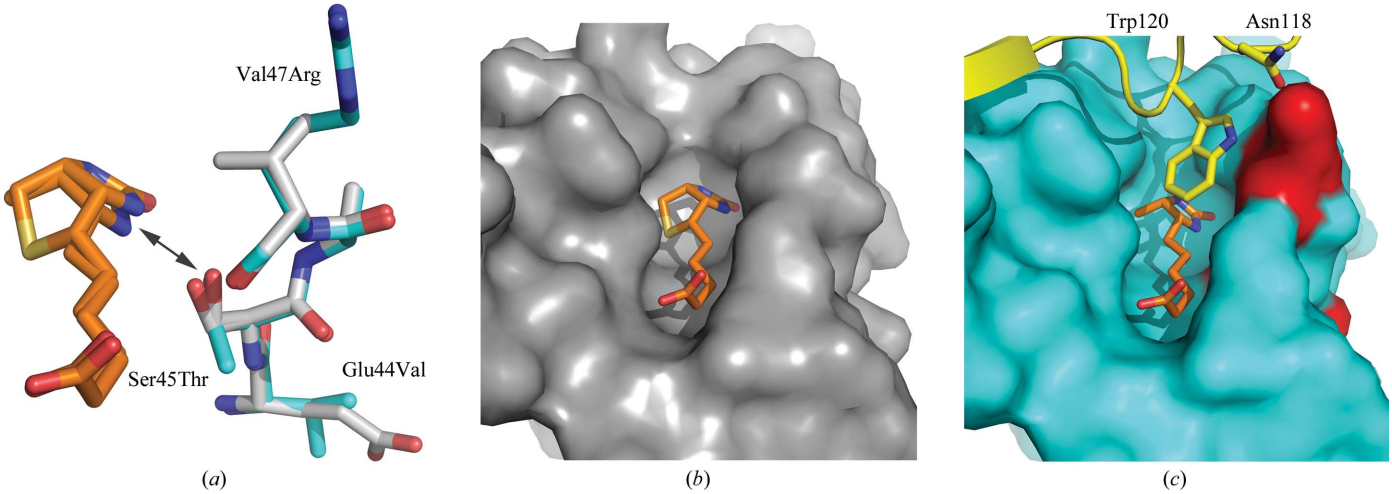


**Figure 3**
A comparison between streptavidin–biotin and *Strep*-Tactin–desthiobiotin complexes. (*a*) The overlay of both binding pockets shows the superposition of biotin with desthiobiotin. Residues 44–47 of *Strep*-Tactin (in cyan) and streptavidin (in grey) are represented and the three mutations Glu44Val, Ser45Thr and Val47Arg are highlighted. Among these, only the side chain of residue 45 points towards the ligand. The arrow indicates that the protein–ligand interaction is similar in both complexes. (*b*) Surface representation of the binding cavity of wild-type streptavidin with biotin. (*c*) Surface representation of the binding cavity of *Strep*-Tactin with desthiobiotin. In addition, residues from the adjacent dimer (same colour code as in Fig. 2), Trp120 and Asn118, which interact with Arg47 are represented. Residues 44, 45 and 47 are shown in red.

Arg53 $N^{\varepsilon}$). Because these two residues are located at both extremities of the flexible loop that moves during ligand binding, their interaction could control the loop movement. Mutation of Glu44 to Val44 prevents any hydrogen-bonding interaction with Arg53 and could thus modify the dynamical properties of the loop. A structure of a multiple mutant engineered to alter desthiobiotin-binding properties in complex with desthiobiotin has recently been published (Magalhães *et al.*, 2011). Interestingly, the authors have identified a mutation Ser52Gly at the base of the flexible loop which slows the dissociation of desthiobiotin. They also identified a series of mutations that enlarge the cavity compared with that of wild-type streptavidin. The residues are located on the opposite ridge of the cavity compared with the *Strep*-Tactin mutations (Fig. 2*c*). Desthiobiotin in the *Strep*-Tactin structure superimposes perfectly with the same ligand in the R7-2 mutant (PDB entry 3rdq; Magalhães *et al.*, 2011).

### 3.3. Elution of *Strep*-Tactin from *Strep*-Tactin matrix

The elution of *Strep*-Tactin from the matrix was assayed using detergents with different alkyl-chain lengths, polar heads and critical micellar concentrations (CMCs; see legend to Fig. 1*c*). With the exception of LAPAO, all of these detergents were described as being compatible with *Strep*-Tactin purification (GE Healthcare application note). For each detergent, two concentrations were assayed: below and above the maximal concentration mentioned in the application note. *Strep*-Tactin could be eluted in all conditions to different extents (Fig. 1*c*), indicating that many of the detergents commonly used for membrane-protein purification are able to release *Strep*-Tactin from the column or the beads. Although the injection order of the detergents was different, the relative magnitudes of the UV-absorbance levels are similar at low and high detergent concentrations. In particular, low *Strep*-Tactin levels were observed at low OG concentration, even though LAPAO was applied first. Similarly, the level of *Strep*-Tactin released at high FC12 concentration is consistent with the level observed at low concentration. These two observations indicate that the elution of *Strep*-Tactin is not influenced by the previous use of LAPAO.

A possible explanation of this release is that most probably not all of the monomers within the tetramer are covalently bound to the resin. Indeed, the exceptional stability of streptavidin tetramers is increased after binding biotin (Sano *et al.*, 1997; Katz, 1997). A single covalent bond could be sufficient to bind whole tetramers to the resin. When binding a *Strep*-Tag II peptide, loop 45–52 is in an open conformation (Korndörfer & Skerra, 2002) and the interaction with Trp120 from the adjacent dimer is weakened. However, the tetramer still exists owing to the hydrophobicity of the dimer–dimer interface (Sano *et al.*, 1997). It might well be the case that detergent molecules disrupt this hydrophobic interface during the course of purification, explaining the release of *Strep*-Tactin from the matrix during elution. During crystallization, *Strep*-Tactin could have been concentrated in a low-detergent phase, favouring the formation of the dimeric hydrophobic interface. The reconstituted tetramers that are reinforced by the presence of desthiobiotin crystallize in the presence of the appropriate precipitant.

## 4. Conclusions

Chromatography based on *Strep*-tag affinity is routinely used for purification of membrane proteins. Although the detergent present in the protein solution does not hinder the binding of *At*NTT1 to the *Strep*-Tactin column, our findings on the effect of detergent on the release of *Strep*-Tactin clearly highlight that such matrices need to be carefully used and that the concept of the stability of streptavidin against mild detergents should be reviewed thoroughly.

We acknowledge access to the beamlines at the European Synchrotron Radiation Facility (ESRF) in Grenoble and to the facilities of the Partnership for Structural Biology (PSB, Grenoble), particularly N-terminal sequencing (IBS) and the nanodrop crystallization robot (HTX-EMBL). We thank Professor Murthy for critical comments on the manuscript. This work was supported in part by the Institut Universitaire de France (grant to EPP) and by the International PhD program Irtelis from CEA (doctoral fellowship for PP).

## References

Cámara-Artigas, A., Hirasawa, M., Knaff, D. B., Wang, M. & Allen, J. P. (2006). *Acta Cryst.* F**62**, 1087–1092.
Caylor, C. L., Dobrianov, I., Lemay, S. G., Kimmer, C., Kriminski, S., Finkelstein, K. D., Zipfel, W., Webb, W. W., Thomas, B. R., Chernov, A. A. & Thorne, R. E. (1999). *Proteins*, **36**, 270–281.
Chilkoti, A., Tan, P. H. & Stayton, P. S. (1995). *Proc. Natl Acad. Sci. USA*, **92**, 1754–1758.
Chivers, C. E., Koner, A. L., Lowe, E. D. & Howarth, M. (2011). *Biochem. J.* **435**, 55–63.
Contreras-Martel, C., Carpentier, P., Morales, R., Renault, F., Chesne-Seck, M.-L., Rochu, D., Masson, P., Fontecilla-Camps, J. C. & Chabrière, E. (2006). *Acta Cryst.* F**62**, 67–69.
Deniaud, A., Bernaudat, F., Frelet-Barrand, A., Juillan-Binard, C., Vernet, T., Rolland, N. & Pebay-Peyroula, E. (2011). *Biochim. Biophys. Acta*, **1808**, 2059–2066.
Deniaud, A., Goulielmakis, A., Covès, J. & Pebay-Peyroula, E. (2009). *PLoS One*, **4**, e6214.
Deniaud, A., Panwar, P., Frelet-Barrand, A., Bernaudat, F., Juillan-Binard, C., Ebel, C., Rolland, N. & Pebay-Peyroula, E. (2012). *PLoS One*, **7**, e32325.
Emsley, P. & Cowtan, K. (2004). *Acta Cryst.* D**60**, 2126–2132.
Hyre, D. E., Le Trong, I., Freitag, S., Stenkamp, R. E. & Stayton, P. S. (2000). *Protein Sci.* **9**, 878–885.
Hyre, D. E., Le Trong, I., Merritt, E. A., Eccleston, J. F., Green, N. M., Stenkamp, R. E. & Stayton, P. S. (2006). *Protein Sci.* **15**, 459–467.
Kabsch, W. (2010). *Acta Cryst.* D**66**, 125–132.
Katz, B. A. (1997). *J. Mol. Biol.* **274**, 776–800.
Korndörfer, I. P. & Skerra, A. (2002). *Protein Sci.* **11**, 883–893.
Lohkamp, B. & Dobritzsch, D. (2008). *Acta Cryst.* D**64**, 407–415.
Magalhães, M. L., Czekster, C. M., Guan, R., Malashkevich, V. N., Almo, S. C. & Levy, M. (2011). *Protein Sci.* **20**, 1145–1154.
McCoy, A. J., Grosse-Kunstleve, R. W., Adams, P. D., Winn, M. D., Storoni, L. C. & Read, R. J. (2007). *J. Appl. Cryst.* **40**, 658–674.
Murshudov, G. N., Skubák, P., Lebedev, A. A., Pannu, N. S., Steiner, R. A., Nicholls, R. A., Winn, M. D., Long, F. & Vagin, A. A. (2011). *Acta Cryst.* D**67**, 355–367.

Reiss-Husson, F. & Picot, D. (1999). *Crystallization of Nucleic Acids and Proteins. A Practical Approach*, edited by A. Ducruix & R. Giégé, pp. 245–268. Oxford University Press.
Sano, T., Vajda, S., Smith, C. L. & Cantor, C. R. (1997). *Proc. Natl Acad. Sci. USA*, **94**, 6153–6158.
Schmidt, T. G. & Skerra, A. (1994). *J. Chromatogr. A*, **676**, 337–345.
Schmidt, T. G. & Skerra, A. (2007). *Nature Protoc.* **2**, 1528–1535.
Veesler, D., Blangy, S., Cambillau, C. & Sciara, G. (2008). *Acta Cryst.* F**64**, 880–885.
Voss, S. & Skerra, A. (1997). *Protein Eng.* **10**, 975–982.
Winn, M. D. *et al.* (2011). *Acta Cryst.* D**67**, 235–242.